

Coherent wiggler radiation impedance at the storage ring cooler for the EIC project

A. Blednykh

September 2022

Electron-Ion Collider
Brookhaven National Laboratory

U.S. Department of Energy

USDOE Office of Science (SC), Nuclear Physics (NP) (SC-26)

Notice: This technical note has been authored by employees of Brookhaven Science Associates, LLC under Contract No. DE-SC0012704 with the U.S. Department of Energy. The publisher by accepting the technical note for publication acknowledges that the United States Government retains a non-exclusive, paid-up, irrevocable, world-wide license to publish or reproduce the published form of this technical note, or allow others to do so, for United States Government purposes.

DISCLAIMER

This report was prepared as an account of work sponsored by an agency of the United States Government. Neither the United States Government nor any agency thereof, nor any of their employees, nor any of their contractors, subcontractors, or their employees, makes any warranty, express or implied, or assumes any legal liability or responsibility for the accuracy, completeness, or any third party's use or the results of such use of any information, apparatus, product, or process disclosed, or represents that its use would not infringe privately owned rights. Reference herein to any specific commercial product, process, or service by trade name, trademark, manufacturer, or otherwise, does not necessarily constitute or imply its endorsement, recommendation, or favoring by the United States Government or any agency thereof or its contractors or subcontractors. The views and opinions of authors expressed herein do not necessarily state or reflect those of the United States Government or any agency thereof.

Coherent wiggler radiation impedance at the storage ring cooler for the EIC project.

A. Blednykh,¹ M. Blaskiewicz,¹ and D. Zhou²

¹Brookhaven National Laboratory, Upton, NY 11973, USA

²KEK, High Energy Accelerator Organization, Oho 1-1, Tsukuba 305-0801, Japan

(Dated: September 15, 2022)

The Electron Ion Collider project is presently under design at Brookhaven National Laboratory. One of the options how to achieve an electron-proton high-luminosity of $10^{34} \text{ cm}^{-2} \text{ s}^{-1}$ range, is the storage ring cooler concept, which is based on employing a significant amount of the damping wigglers. One of the main concerns, in achieving the required beam parameters, is the collective effects, especially the coherent synchrotron radiation impedance produced by the damping wigglers and its effect on the longitudinal beam dynamics. Low energy of the electrons, $E_0=149.6 \text{ MeV}$, small vacuum chamber aperture, $b=15 \text{ mm}$, small bending radius and a big number of poles make the coherent synchrotron radiation simulations for the damping wiggler with D. Zhou's CSRZ code, pretty challenging. The obtained numerical results have been compare with a theoretical approach of Stupakov and Zhou. The strong narrow-band impedance, due to a presence of the periodic poles and the vacuum chamber, have been identified and classified. To suppress or detune the high-Q resonance peaks, a design of the damping wiggler with a varied period of length is presented and discussed.

INTRODUCTION

The storage ring cooler concept for the EIC project has been discussed in Ref. [1]. Because of the emittance growth of the proton beam due to IBS effect during the long collision period, the electron beam requires to be with high intensity to provide the reliable cooling performance. The ring cooler is based on a big amount of the damping wigglers to achieve the required emittance goals. Contribution of the coherent wiggler radiation to the total impedance of the ring can be significant. Low beam energy and high electron beam intensity make the ring more challenging in design from the collective effects stand point. The main ring cooler parameters for the collective effects simulations are presented in Table 1.

Table 1: Main ring cooler parameters.

Energy, E_0	MeV	149.26
Circumference, C	m	426
Momentum compaction, α_c		-3.21×10^{-3}
Revolution period, T_0	μs	1.42
Energy loss, U_0	keV	13.162
Synchrotron tune, ν_s		0.0034
Damping time, σ_x, σ_τ	ms	31.7, 15.71
RF voltage, V_{rf}	kV	28
RF frequency, f_{rf}	MHz	98.5233
Harmonic number, h		140
Energy spread, σ_δ		6.5×10^{-4}
Bunch Length, σ_s	mm	41
Average Current, I_{av}	A	4.4

In this paper, we discuss analysis of the CSR impedance of the damping wiggler with a constant period λ_w , where the real and imaginary parts of the longitudinal impedances are simulated using the CSRZ code

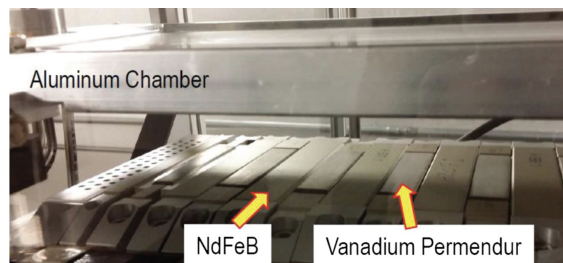


FIG. 1: A partial view of the bottom magnet array of the DW with the Aluminum vacuum chamber.

[2] and the output data are compared with the analytical results using the analytical approach of ref. [3].

DW WITH A CONSTANT PERIOD

Stupakov and Zhou [3] have presented an analytical approach of the real part of the CSR impedance for the damping wiggler with the vacuum chamber as

$$\text{Re}Z(k) = 4Z_0\theta_0^2 F(k), \quad (1)$$

where

$$F(k) = \frac{k_w^2}{abk} \times \sum_{n_1, n_2} \frac{1}{k_z} \left(\frac{k^2 k_y^2}{\varkappa^2 (1 + \delta_{0, n_1})} + k_x^2 \left(\frac{k_z}{\varkappa} - \frac{\varkappa}{k - k_z} \right)^2 \right) \times \frac{\sin^2[\pi N_p (k - k_z)/k_w]}{[(k - k_z)^2 - k_w^2]^2}, \quad (2)$$

$\theta_0 = K/\gamma$ is the maximal deflection angle, $K \approx 93.4 B_w \lambda_w$ is the damping wiggler parameter with B_w

the wiggler magnetic field and λ_w the wiggler period, $\gamma = E_0/E_{e-}$, is the Lorentz factor, $k_x = \frac{\pi n_1}{a}$, $k_y = \frac{\pi n_2}{b}$, $\varkappa = \sqrt{k_x^2 + k_y^2}$, $k_z = \sqrt{k^2 - \varkappa^2} > 0$, and $k_w = \frac{2\pi}{\lambda_w}$ are the horizontal, vertical and longitudinal wave numbers, δ is the Kronecker delta.

Eq. (2) is an approximation of the wiggler radiation impedance for the first harmonic of beam motion, where the waveguide modes are in synchronism with the beam motion and only the waveguide modes with even n_1 and odd n_2 can be synchronized with the $p = 1$ harmonic. Therefore, the summation in Eq. (2) is for $n_1=0, 2, 4, 6, \dots$, and $n_2=1, 3, 5, 7, \dots$. The synchronization function in Eq. (2) is essential in defining the feature of impedance spectrum. When the number of period N_p is large, the impedance spectrum is highly peaked at k satisfying

$$k - k_z = k_w. \quad (3)$$

In Ref. [2], a more general resonance condition was found to be

$$k - k_z = pk_w, \quad (4)$$

with $p \leq 1$ the harmonic number of beam oscillation when traversing the wiggler. The resonance frequencies are found at

$$k_{n_1, n_2} = \frac{p^2 k_w^2 + \varkappa^2}{2pk_w}. \quad (5)$$

Usually $p = 1$ terms dominate the impedance spectrum.

The real (Fig. 2) and imaginary (Fig. 3) parts of the CSR impedance for the damping wiggler with a constant period are plotted for $E_0 = 149.8$ MeV, $B_w = 1.9$ T, $\lambda_w = 0.048$ m, $N_p = 158$, $b = 15$ mm and $a = 45$ mm, where b and a are the full vertical and horizontal apertures of the vacuum chamber (Table 2). The red trace are the data numerically simulated by Demin Zhou's CSRZ code. The gray trace is the result due to analytical approximation of Eq. (1) (Two parallel metal plates model). As can be seen, the results are shifted relative to each other by 3 GHz. The difference can be explained as follows: the CSRZ code solves the parabolic equation instead of the full Maxwell's equations. For the problem of wiggler radiation, the paraxial approximation implies taking the approximation of

$$k - k_z \approx \frac{\varkappa^2}{2k}. \quad (6)$$

With the above approximation, the resonant frequencies predicted by CSRZ will be

$$k_{n_1, n_2}^{CSRZ} = \frac{\varkappa^2}{2pk_w}. \quad (7)$$

For $p = 1$, the peak positions will be shifted by an amount of $k_w/2$, which corresponds to $\Delta f \approx 3.1$ GHz with the parameters listed above for Fig 2.

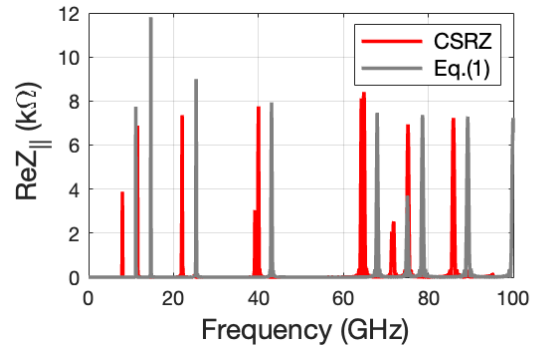


FIG. 2: Real part of the longitudinal impedance for DW with the constant period length.

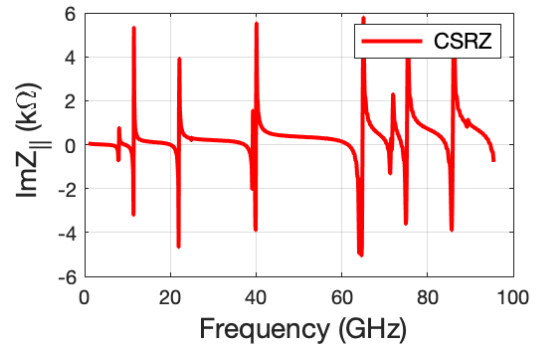


FIG. 3: Imaginary part of the longitudinal impedance for DW with the constant period length.

All resonance modes are identified and classified and they all correspond to H-Mode. The first lowest mode in a rectangular vacuum chamber with $H_z \neq 0$ and $E_z = 0$ and $n_1 = 0, 2, 4, 6, \dots$, and $n_2 = 1, 3, 5, 7, \dots$, can be classified as H_{01} -mode and its generated at frequency $f_1=11.1$ GHz with $a=45$ mm and $b=15$ mm. Hence the next generated modes are H_{21} -Mode, H_{41} -Mode and H_{61} -Mode at frequencies $f_2=14.6$ GHz, $f_3=25.3$ GHz and $f_4=43.1$ GHz respectively. The electric and magnetic field pattern of the first two modes, H_{01} -Mode and H_{21} -Mode, are shown in Fig. 4.

Table 2: Damping wiggler and chamber parameters.

Magnetic field, B	T	2.8
Length, L	m	7.44
Bending radius, ρ	m	0.246
Wiggler period, λ_w	mm	48
Number of poles, N_p		155
Vertical aperture, b	mm	15
Horizontal aperture, a	mm	45

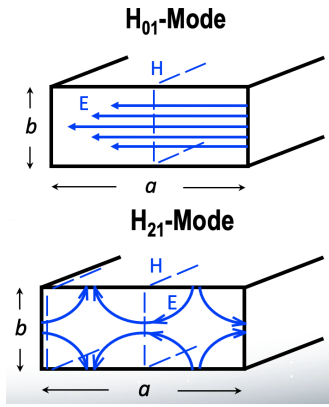


FIG. 4: Electric and magnetic fields pattern of H_{01} -Mode and H_{21} -Mode in a rectangular waveguide.

DW WITH A VARIED PERIOD (DETUNED)

To suppress the narrow-band impedance, a new DW design with a varied period length along the beam direction is discussed. The main idea is to spread the resonance frequencies of each particular mode via the small change in period length. In this case a high-Q peak becomes broader and gets smaller in magnitude. This method was first developed and applied for HOM suppression in the multi-cells accelerator structures [5], where each neighboring cavity is differed in dimensions (radius and length) from the previous one. This method is more convenient for DW, since we don't need to concern about the fundamental mode like in the accelerating structure. In the numerical simulations, the DW period length is varied as $\lambda_i = \lambda_w + (i - 1)\Delta\lambda$, where $i=1, 2, 3, \dots, N_p$. The number of periods is $N_p=141$ and the difference between following periods is $\Delta\lambda=70 \mu m$. These parameters were chosen to keep the total length close to the length of the DW with the constant period. The total difference between the last and the first period length is within $\sim 20 \%$, and it is changed from $\lambda_1=48 \text{ mm}$ to $\lambda_{141}=58 \text{ mm}$. The real and imaginary parts of the longitudinal impedance for DW with varied (blue trace) and constant period (red trace) are presented in Fig. 5 and Fig. 6 (blue trace). The narrow-band impedance has been tremendous suppressed due to the frequencies spread.

SUMMARY

The work on CSR DW impedance optimization is continued. Based on the simulated results of $ReZ_{||}(k)$ and $ImZ_{||}(k)$, we were able to reconstruct the wakefield and apply it for the beam dynamics simulations. The next step is to simulate the collective effects and check the in-

stability threshold dependence on the different DW vac-

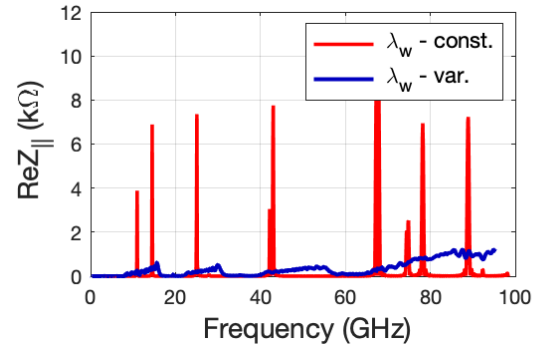


FIG. 5: Real part of the longitudinal impedance for the DW with constant and varied period lengths.

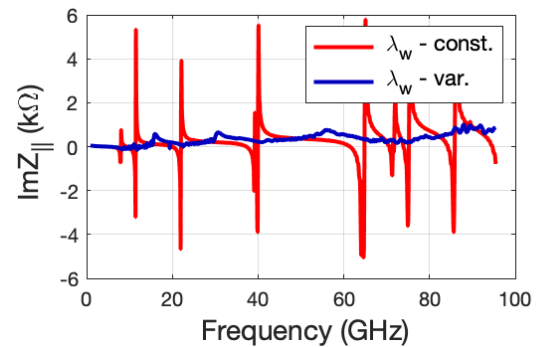


FIG. 6: Imaginary part of the longitudinal impedance for the DW with constant and varied period lengths.

uum chamber gaps. Simulating this very narrow resonance impedance with the ELEGANT code will be challenging task.

-
- [1] H. Zhao, J. Kewisch, M. Blaskiewicz, and A. Fedotov, Phys. Rev. Accel. Beams 24, 043501 (2021) - Published 5 April 2021
 - [2] D. Zhou, "Coherent Synchrotron Radiation and Microwave Instability in Electron Storage Rings", Ph.D. thesis, SOKENDAI and KEK, 2011.
 - [3] G. Stupakov and D. Zhou, "Longitudinal impedance due to coherent undulator radiation in a rectangular waveguide", SLAC-PUB-14332, December 9, 2010.
 - [4] G. Stupakov and D. Zhou, "Analytical theory of coherent synchrotron radiation wakefield of short bunches shielded by conducting parallel plates", Phys. Rev. Accel. Beams 19, 044402 (2016) - Published 21 April 2016.
 - [5] H. Derugter, Z. D. Farkas, H. A. Hoag, K. Ko, N. Kroll, G. A. Loew, R. Miller, R. B. Palmer, J. M. Paterson, K. A. Thompson, J. W. Wang, P. B. Wilson, "Damped and detuned accelerator structures", SLAC-PUB-5322, September 1990.